function in an androgen-independent mechanism. It is known that a number of coactivators function as general coactivators for transcription mediated by nuclear receptors. For example RBM14 is known to activate glucocorticoid receptor-, estrogen receptor-, and thyroid hormone receptor-mediated transcription [59]. It has been reported that SFPQ regulates progesterone receptor, thyroid hormone receptor and retinoic acid receptor, suggesting that SFPQ is a general coregulator of nuclear receptors [24, 25]. In germ cells, several specific nuclear receptors are expressed [60, 61]. PSPC1 and SFPQ may regulate transcription mediated by another nuclear receptor in germ cells. Sertoli cells regulate highly organized and precisely synchronized germ cell development by nourishing the germ cells via their secretion products. Activity of AR-mediated transcription in Sertoli cells is regulated by multiple coregulators. Our present study suggests that the DBHS-containing proteins are coactivators of AR transactivation in Sertoli cells and may be determinants of androgen activity during spermatogenesis. In conclusion, PSPC1, NONO, and SFPQ may support spermatogenesis by regulating androgen receptor-mediated transcription in Sertoli cells.

ACKNOWLEDGMENTS

We thank Dr. Naohito Nozaki for antibody production, and M.S. Atsushi Kawaguchi for his helpful discussion.

REFERENCES

1. Russell LD, Ettlin RA, Sinha Hikim AP, Clegg ED. Histological and Histopathological Evaluation of the Testis. Clearwater, FL: Cache River Press; 1990:1–40.
2. Maclean JA 2nd, Wilkinson MF. Gene regulation in spermatogenesis. Curr Top Dev Biol 2005; 71:131–197.
3. Tanaka H, Baba T. Gene expression in spermiogenesis. Cell Mol Life Sci 2005; 62:344–354.
4. Monaco L, Kotaja N, Fienga G, Hogeveen K, Kolthur US, Kimmins S, Brancorsini S, Macho B, Sassone-Corsi P. Specialized rules of gene transcription in male germ cells: the CREM paradigm. Int J Androl 2004; 27:322–327.
5. Kimmins S, Kotaja N, Davidson I, Sassone-Corsi P. Testis-specific transcription mechanisms promoting male germ-cell differentiation. Reproduction 2004; 128:5–12.
6. Kashiwabara S, Noguchi J, Zhuang T, Ohmura K, Honda A, Sugiura S, Miyamoto K, Takahashi S, Inoue K, Ogura A, Baba T. Regulation of spermatogenesis by testis-specific, cytoplasmic poly(A) polymerase TPAP. Science 2002; 298:1999–2002.
7. Mruk DD, Cheng CY. Sertoli-Sertoli and Sertoli-germ cell interactions and their significance in germ cell movement in the seminiferous epithelium during spermatogenesis. Endocr Rev 2004; 25:747–806.
8. Griswold MD. The central role of Sertoli cells in spermatogenesis. Semin Cell Dev Biol 1998; 9:411–416.
9. Syed V, Hecht NB. Disruption of germ cell-Sertoli cell interactions leads to spermatogenic defects. Mol Cell Endocrinol 2002; 186:155–157.
10. Dohle GR, Smit M, Weber RF. Androgens and male fertility. World J Urol 2003; 21:341–345.
11. Chang C, Chen YT, Yeh SD, Xu Q, Wang RS, Guillou F, Lardy H, Yeh S. Infertility with defective spermatogenesis and hypotestosteronemia in male mice lacking the androgen receptor in Sertoli cells. Proc Natl Acad Sci U S A 2004; 101:6876–6881.
12. De Gendt K, Swinnen JV, Saunders PT, Schoonjans L, Dewerchin M, Devos A, Tan K, Atanassova N, Claessens F, Lecureuil C, Heyns W, Carmeliet P, Guillou F, Sharpe RM, Verhoeven G. A Sertoli cell-selective knockout of the androgen receptor causes spermatogenic arrest in meiosis. Proc Natl Acad Sci U S A 2004; 101:1327–1332.
13. Kato S, Matsumoto T, Kawano H, Sato T, Takeyama K. Function of androgen receptor in gene regulations. J Steroid Biochem Mol Biol 2004; 89–90:627–633.
14. Yong EL, Loy CJ, Sim KS. Androgen receptor gene and male infertility. Hum Reprod Update 2003; 9:1–7.
15. Kato S, Sato T, Watanabe T, Takemasa S, Masuhiro Y, Ohtake F, Matsumoto T. Function of nuclear sex hormone receptors in gene regulation. Cancer Chemother Pharmacol 2005; 56:4–9.
16. MacLean HE, Warne GL, Zajac JD. Localization of functional domains in the androgen receptor. J Steroid Biochem Mol Biol 1997; 62:233–242.
17. Heinlein CA, Chang C. Androgen receptor (AR) coregulators: an overview. Endocr Rev 2002; 23(2):175–200.
18. Wang L, Hsu CL, Chang C. Androgen receptor corepressors: an overview. Prostate 2005; 63:117–130.
19. McEwan IJ. Molecular mechanisms of androgen receptor-mediated gene regulation: structure-function analysis of the AF-1 domain. Endocr Relat Cancer 2004; 11:281–293.
20. Ishitani K, Yoshida T, Kitagawa H, Ohta H, Nozawa S, Kato S. p54nrb acts as a transcriptional coactivator for activation function 1 of the human androgen receptor. Biochem Biophys Res Commun 2003; 306:660–665.
21. Ishiguro H, Uemura H, Fujinami K, Ikeda N, Ohta S, Kubota Y. 55 kDa nuclear matrix protein (nmt55) mRNA is expressed in human prostate cancer tissue and is associated with the androgen receptor. Int J Cancer 2003; 105:26–32.
22. Fox AH, Lam YW, Leung AK, Lyon CE, Andersen J, Mann M, Lamond AI. Paraspeckles: a novel nuclear domain. Curr Biol 2002; 12:13–25.
23. Shav-Tal Y, Zipori D. PSF and p54(nrb)/NonO–multi-functional nuclear proteins. FEBS Lett 2002; 531:109–114.
24. Dong X, Shylnova O, Challis JR, Lye SJ. Identification and characterization of the protein-associated splicing factor as a negative co-regulator of the progesterone receptor. J Biol Chem 2005; 280:13329–13340.
25. Mathur M, Tucker PW, Samuels HH. PSF is a novel corepressor that mediates its effect through Sin3A and the DNA binding domain of nuclear hormone receptors. Mol Cell Biol 2001; 21:2298–2311.
26. Gozani O, Patton JG, Reed R. A novel set of spliceosome-associated proteins and the essential splicing factor PSF bind stably to pre-mRNA prior to catalytic step II of the splicing reaction. EMBO J 1994; 13:3356–3367.
27. Rosonina E, Ip JY, Calarco JA, Bakowski MA, Emili A, McCracken S, Tucker P, Ingles CJ, Blencowe BJ. Role for PSF in mediating transcriptional activator-dependent stimulation of pre-mRNA processing in vivo. Mol Cell Biol 2005; 25:6734–6746.
28. Liang S, Lutz CS. p54nrb is a component of the snRNP-free U1A (SF-A) complex that promotes pre-mRNA cleavage during polyadenylation. RNA 2006; 12:111–121.
29. Zhang Z, Carmichael GG. The fate of dsRNA in the nucleus: a p54(nrb)-containing complex mediates the nuclear retention of promiscuously A-to-I edited RNAs. Cell 2001; 106:465–75.
30. Kanai Y, Dohmae N, Hirokawa N. Kinesin transports RNA: isolation and characterization of an RNA-transporting granule. Neuron 2004; 43:513–525.
31. Straub T, Grue P, Uhse A, Lisby M, Knudsen BR, Tange TO, Westergaard O, Boege F. The RNA-splicing factor PSF/p54 controls DNA-topoisomerase I activity by a direct interaction. J Biol Chem 1998; 273:26261–26264.
32. Bladen CL, Udayakumar D, Takeda Y, Dynan WS. Identification of the polypyrimidine tract binding protein-associated splicing factor p54(nrb) complex as a candidate DNA double-strand break rejoining factor. J Biol Chem 2005; 280:5205–5210.
33. Powers CA, Mathur M, Raaka BM, Ron D, Samuels HH. TLS (translocated-in-liposarcoma) is a high-affinity interactor for steroid, thyroid hormone, and retinoid receptors. Mol Endocrinol 1998; 12:4–18.
34. Iacobazzi V, Infantino V, Costanzo P, Izzo P, Palmieri F. Functional analysis of the promoter of the mitochondrial phosphate carrier human gene: identification of activator and repressor elements and their transcription factors. Biochem J 2005; 391:613–621.
35. Deloulme JC, Prichard L, Delattre O, Storm DR. The prooncoprotein EWS binds calmodulin and is phosphorylated by protein kinase C through an IQ domain. J Biol Chem 1997; 272:27369–27377.
36. Adegbola O, Pasternack GR. A pp32-retinoblastoma protein complex modulates androgen receptor-mediated transcription and associates with components of the splicing machinery. Biochem Biophys Res Commun 2005; 334:702–708.
37. Zhang WW, Zhang LX, Busch RK, Farres J, Busch H. Purification and characterization of a DNA-binding heterodimer of 52 and 100 kDa from HeLa cells. Biochem J 1993; 290:267–272.
38. Zolotukhin AS, Michalowski D, Bear J, Smulevitch SV, Traish AM, Peng R, Patton J, Shatsky IN, Felber BK. PSF acts through the human immunodeficiency virus type 1 mRNA instability elements to regulate virus expression. Mol Cell Biol 2003; 23:6618–6630.
39. Xu J, Zhong N, Wang H, Elias JE, Kim CY, Woldman I, Pifl C, Gygi SP, Geula C, Yankner BA. The Parkinson's disease-associated DJ-1 protein is a transcriptional co-activator that protects against neuronal apoptosis. Hum Mol Genet 2005; 14:1231–1241.
40. Emili A, Shales M, McCracken S, Xie W, Tucker PW, Kobayashi R,

Blencowe BJ, Ingles CJ. Splicing and transcription-associated proteins PSF and p54nrb/nonO bind to the RNA polymerase II CTD. RNA 2002; 8:1102–1111.
41. Myojin R, Kuwahara S, Yasaki T, Matsunaga T, Sakurai T, Kimura M, Uesugi S, Kurihara Y. Expression and functional significance of mouse paraspeckle protein 1 on spermatogenesis. Biol Reprod 2004; 71:926–932.
42. Fox AH, Bond CS, Lamond AI. P54nrb Forms a Heterodimer with PSP1 That Localizes to Paraspeckles in an RNA-dependent Manner. Mol Biol Cell 2005; 16:5304–5315.
43. Suzuki T, Kitamura S, Khota R, Sugihara K, Fujimoto N, Ohta S. Estrogenic and antiandrogenic activities of 17 benzophenone derivatives used as UV stabilizers and sunscreens. Toxicol Appl Pharmacol 2005; 203:9–17.
44. Novy M, Pohn R, Andorfer P, Novy-Weiland T, Galos B, Schwarzmayr L, Rotheneder H. EAPP, a novel E2F binding protein that modulates E2F-dependent transcription. Mol Biol Cell 2005; 16:2181–2190.
45. Takahashi S, Inatome R, Yamamura H, Yanagi S. Isolation and expression of a novel mitochondrial septin that interacts with CRMP/CRAM in the developing neurones. Genes Cells 2003; 8:81–93.
46. Tabuchi Y, Ohta S, Yanai N, Obinata M, Kondo T, Fuse H, Asano S. Development of the conditionally immortalized testicular Sertoli cell line TTE3 expressing Sertoli cell specific genes from mice transgenic for temperature sensitive simian virus 40 large T antigen gene. J Urol 2002; 167:1538–1545.
47. Dai T, Vera Y, Salido EC, Yen PH. Characterization of the mouse Dazap1 gene encoding an RNA-binding protein that interacts with infertility factors DAZ and DAZL. BMC Genomics 2001; 2:6.
48. Kurihara Y, Watanabe H, Kawaguchi A, Hori T, Mishiro K, Ono M, Sawada H, Uesugi S. Dynamic changes in intranuclear and subcellular localizations of mouse Prrp/DAZAP1 during spermatogenesis: the necessity of the C-terminal proline-rich region for nuclear import and localization. Arch Histol Cytol 2004; 67:325–333.
49. Sharpe RM, McKinnell C, Kivlin C, Fisher JS. Proliferation and functional maturation of Sertoli cells, and their relevance to disorders of testis function in adulthood. Reproduction 2003; 125:769–784.
50. Meissner M, Dechat T, Gerner C, Grimm R, Foisner R, Sauermann G. Differential nuclear localization and nuclear matrix association of the splicing factors PSF and PTB. J Cell Biochem 2000; 76:559–566.
51. Shav-Tal Y, Lee B, Bar-Haim S, Vandekerckhove J, Zipori D. Enhanced proteolysis of pre-mRNA splicing factors in myeloid cells. Exp Hematol 2000; 28:1029–1038.
52. Traish AM, Huang YH, Ashba J, Pronovost M, Pavao M, McAneny DB, Moreland RB. Loss of expression of a 55 kDa nuclear protein (nmt55) in estrogen receptor-negative human breast cancer. Diagn Mol Pathol 1997; 6:209–221.
53. Boonyaratanakornkit V, Melvin V, Prendergast P, Altmann M, Ronfani L, Bianchi ME, Taraseviciene L, Nordeen SK, Allegretto EA, Edwards DP. High-mobility group chromatin proteins 1 and 2 functionally interact with steroid hormone receptors to enhance their DNA binding in vitro and transcriptional activity in mammalian cells. Mol Cell Biol 1998; 18:4471–4487.
54. Jeong BC, Hong CY, Chattopadhyay S, Park JH, Gong EY, Kim HJ, Chun SY, Lee K. Androgen receptor corepressor-19 kDa (ARR19), a leucine-rich protein that represses the transcriptional activity of androgen receptor through recruitment of histone deacetylase. Mol Endocrinol 2004; 18:13–25.
55. Ozanne DM, Brady ME, Cook S, Gaughan L, Neal DE, Robson CN. Androgen receptor nuclear translocation is facilitated by the f-actin cross-linking protein filamin. Mol Endocrinol 2000; 14:1618–1626.
56. Schrantz N, da Silva Correia J, Fowler B, Ge Q, Sun Z, Bokoch GM. Mechanism of p21-activated kinase 6-mediated inhibition of androgen receptor signaling. J Biol Chem 2004; 279:1922–1931.
57. Yang YS, Yang MC, Tucker PW, Capra JD. NonO enhances the association of many DNA-binding proteins to their targets. Nucleic Acids Res 1997; 25:2284–2292.
58. Kiesler E, Miralles F, Ostlund Farrants AK, Visa N. The Hrp65 self-interaction is mediated by an evolutionarily conserved domain and is required for nuclear import of Hrp65 isoforms that lack a nuclear localization signal. J Cell Sci 2003; 116:3949–3956.
59. Iwasaki T, Chin WW, Ko L. Identification and characterization of RRM-containing coactivator activator (CoAA) as TRBP-interacting protein, and its splice variant as a coactivator modulator (CoAM). J Biol Chem 2001; 276:33375–33383.
60. Hummelke GC, Cooney AJ. Reciprocal regulation of the mouse protamine genes by the orphan nuclear receptor germ cell nuclear factor and CREMtau. Mol Reprod Dev 2004; 68:394–407.
61. Lee CH, Chinpaisal C, Wei LN. A novel nuclear receptor heterodimerization pathway mediated by orphan receptors TR2 and TR4. J Biol Chem 1998; 273:25209–25215.

Identification of prostatic-secreted proteins in mice by mass spectrometric analysis and evaluation of lobe-specific and androgen-dependent mRNA expression

Nariaki Fujimoto, Yukimi Akimoto[1], Tomoharu Suzuki[2], Shigeyuki Kitamura[2] and Shigeru Ohta[2]

Department of Developmental Biology, Research Institute for Radiation Biology and Medicine, Hiroshima University, 1-2-3 Kasumi, Minami-ku, Hiroshima 734-8553, Japan

[1]Department of Radiation Responses, Research Institute for Radiation Biology and Medicine, Hiroshima University, 1-2-3 Kasumi, Minami-ku, Hiroshima 734-8553, Japan

[2]Department of Xenobiotic Metabolism and Molecular Toxicology, Institute of Pharmaceutical Sciences, Hiroshima University School of Medicine, Kasumi 1-2-3, Minami-ku, Hiroshima 734-8551, Japan

(Requests for offprints should be addressed to N Fujimoto; Email: nfjm@hiroshima-u.ac.jp)

Abstract

Rats and guinea pigs have frequently been used to study the development of the prostate and the mechanism of androgen action, but the mouse prostate has also become an attractive model for prostate research, because an enormous range of genetically altered mice is now available. However, the secretion of proteins in the mouse prostate has not yet been thoroughly investigated. In the present study, major secreted proteins from the ventral prostate (VP), dorsolateral prostate (DLP), and anterior prostate (AP) of mice were identified by means of 2D-gel electrophoresis followed by MALDI-TOF mass spectrometric analysis. A quantitative reverse transcriptase-PCR method was further employed to examine the androgen-dependent transcriptional regulation of the identified proteins. Proteome analysis revealed that the VP secretes spermine-binding protein, serine protease inhibitor Kazal type-3, and a 91 kDa hypothetical scavenger receptor (AK035662). DLP and AP secrete a protein similar to immunoglobulin-binding protein, immunoglobulin-binding protein-like protein, and one of the experimental autoimmune prostatitis antigen proteins (EAPA2). Peroxiredoxin-6, glucose-regulated protein 78, zinc-α2-glycoprotein, and phospholipase Cα are also secreted. Castration of animals led to a decrease in the mRNAs of these secreted proteins, although the extents of changes varied greatly among different lobes. We present here an outlined view of mouse prostate secretion, which should contribute to an understanding of the biological functions of the prostate gland, as well as the androgen dependency of prostate secretion.

Journal of Endocrinology (2006) **190,** 793–803

Introduction

Rat models have been widely used to study prostate morphology, development, and pathology, as well as androgen-regulated gene expression, in order to understand the basic functions and pathology of this male accessory sex gland (Cunha *et al.* 1987). Mice have generally not been used because the small size of the gland makes morphological studies difficult, and because the mouse prostate is less susceptible to carcinogenesis (Shirai *et al.* 2000). Recently, however, a huge range of transgenic and knockout mice has become available with considerable potential for studies of the prostate (Abate-Shen & Shen 2002, Klein 2005). Transgenic adenocarcinoma of the mouse prostate (TRAMP) mice has been used to study the progression and chemoprevention of prostate cancer (Greenberg *et al.* 1995). Prolactin transgenic mice have been used to investigate the effect of prolactin on prostate growth (Wennbo *et al.* 1997). Estrogen receptor knockout mice (αERKO and βERKO) have been used to examine the role of estrogen in prostate development (Weihua *et al.* 2001, Omoto *et al.* 2005). Aromatase knockout, prolactin receptor knockout, and conditional deletion of Rb mice have been used to study the involvement of those genes in prostate carcinogenesis (McPherson *et al.* 2001, Robertson *et al.* 2003, Maddison *et al.* 2004). However, despite these recent developments, the basic biological function of the prostate, prostatic secretion, is still poorly understood in the mouse. Identification of the secreted proteins will be helpful in understanding prostate development and pathology.

The rodent prostate consists of the ventral prostate (VP), lateral prostate (LP), dorsal prostate (DP), and anterior prostate (AP or coagulating gland). It is well known that rat prostatic secretory proteins, such as prostatein and cystatin-related protein, are mainly produced in the VP, and other proteins, such as prostatic secretory protein of 94 aa (PSP94), probasin,

Journal of Endocrinology (2006) **190,** 793–803
0022–0795/06/0190–793
DOI: 10.1677/joe.1.06733
Online version via http://www.endocrinology-journals.org

and seminal vesicle secretion 2 (SVS2) are abundant in the LP and DP (Cunha *et al.* 1987). An early study revealed that spermine-binding protein (SBP) and serine protease inhibitor Kazal type-3 (SPI-KT3) are abundant in the mouse VP (Mills *et al.* 1987*a*, 1987*b*). Proteins secreted from the dorso-lateral prostate (DLP) and AP have not yet been identified, although Cunha's group developed a specific polyclonal antibody for major DLP protein(s) to be used as a differentiation marker (Donjacour *et al.* 1990).

In the present study, the major proteins secreted from the VP, DLP, and AP were identified by means of 2D-gel electrophoresis followed by MALDI-TOF mass spectrometric analysis. Further, a quantitative reverse transcriptase (RT)-PCR method was employed to examine the androgen dependence of the transcriptional regulation of the secretory proteins.

Materials and Methods

Animals

Animal experiments were conducted in accordance with *A Guide for the Care and Use of Laboratory Animals of Hiroshima University.* The male C57BL mice were purchased from Charles River Japan Co. (Kanagawa, Japan) and maintained with free access to basal diet and tap water. For proteome analysis, three of the 11-week-old mice were killed under ether anesthesia and the prostate and seminal vesicle (SV) were carefully dissected out. In addition, four animals were used for evaluating the sample preparation method. For the study of age-dependent mRNA expression, animals were killed at 1, 2, 4, 6, and 11 weeks (four animals per group), and each of the prostate lobes was dissected under a microscope and immediately fixed in RNA Later solution (Ambion, Inc., Austin, TX, USA). For the castration and hormone-replacement study, animals were divided into three groups, the castrated, castrated plus testosterone injected, and intact. Surgical castration was made at 10 weeks of age and animals were allowed to recover for 1 week. Testosterone propionate (Wako Junyaku KK, Osaka, Japan) was dissolved in the vehicle oil, Panacete 810 (Nippon Oils and Fats Co., Ltd, Tokyo, Japan), and the solution was administered i.p. at a dose of 5 mg/kg body weight. Animals were killed under ether anesthesia 24 h after testosterone injection, and the prostate lobes were collected for RNA extraction.

Preparation of secretion samples

Preparation of secretion samples was performed based on the previously reported method (Donjacour *et al.* 1990). Each dissected prostate lobe from an 11-week-old mouse was rinsed well in saline and placed on a 35 mm culture dish with 100 µl saline containing 1% protease inhibitor mixture (Sigma). Each lobe was cut into four or five pieces, left to stand for 5 min, and transferred to a 1·5 ml microcentrifuge tube. After centrifugation at 10 000 *g* for 5 min at room temperature, the supernatant was collected as the secretion sample. The incubation time of 5 min was chosen because inner cellular contamination (glyceraldehyde-3-phosphate dehydrogenase; GAPDH) was confirmed to below by 5 min (Fig. 1). For the SV secretion sample, the content of the vesicle was collected and suspended in saline with protease inhibitors. The protein concentration of each sample solution was determined with a Protein Assay kit (Bio-Rad Lab.). For de-glycosidation, samples were incubated with PNGase F (50 U/µg protein; New England Biolabs, Ipswich, MA, USA) at 37 °C for 1·5 h.

Electrophoresis (1D and 2D-PAGE)

For SDS-PAGE gel electrophoresis, 15 µg total protein of each sample were mixed with the SDS-PAGE buffer containing 2-mercaptoethanol, and applied to a 5–20% gradient PAGE gel (10×10 cm^2 SuperSep pre-cast gel; Wako Jyunyaku) with molecular weight markers, Precision Plus (Bio-Rad Lab.). The electrophoresis was carried out at a constant current of 20 mA. The gel was fixed and stained with 45% methanol and 10% acetic acid containing 0·2% Coomassie Brilliant Blue, followed by de-staining with 7% methanol and 7% acetic acid.

For 2D-gel electrophoresis, 1D isoelectric focusing with immobilized pH gradients was performed with Immobiline

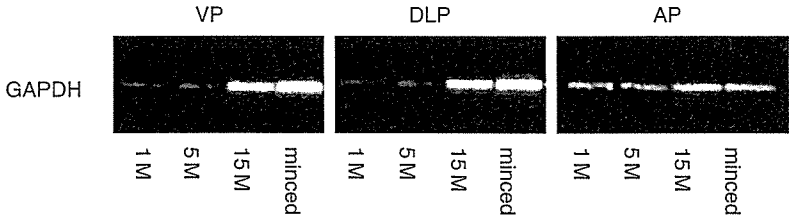

Figure 1 Intracellular contamination in secretion samples. Each prostatic lobe was cut into four or five pieces, and secretion out of the prostatic canals was allowed for 1, 5, and 15 min. Then the lobes were centrifuged and the supernatant was collected as the secretion sample. The samples were applied to the SDS-PAGE (5–20%) at 0·3 µg protein/lane, transferred to a piece of PVDF membrane and immunostained with antibody to GAPDH, an inner cellular marker (36 kDa band). The intracellular contamination was lesser in the samples incubated for 1 and 5 min (1, 5 M) than in those incubated for 15 min (15 M) or prepared from minced tissues (minced). The incubation time of 5 min was chosen for sample preparation in the present study.

DryStrip (Amersham) and the Ettan IPGphor system (Amersham) according to the manufacturer's protocol. For analytical 2D-PAGE, 10 μg de-glycosidated protein was applied in a 7 cm Immobiline DryStrip (pI 3–11, nonlinear gradient). After rehydration, the strip was isoelectrofocused (15 kVh). The Immobiline gel was then treated with SDS equilibration buffer (50 mM Tris–HCl, pH 8·8, 6 M urea, 30% glycerol, and 2% SDS) containing 10 mg/ml DTT for 15 min, followed by the same buffer containing 25 mg/ml iodoacetamide. The Immobiline gel was then placed on the second SDS-PAGE slab gel with 5–20% gradient (SuperSep pre-cast gel, Wako Jyunyaku) and overlaid with hot agarose solution to connect the two gels. The second electrophoresis was run at a constant current of 20 mA. The gel was fixed with 50% methanol and 7% acetic acid, stained overnight in Sypro Ruby (Invitrogen), and de-stained with 10% methanol and 7% acetic acid. Stained gels were scanned with a Molecular Imager FX Pro (Bio-Rad Lab.), with excitation at 532 nm. In the case of preparative 2D-PAGE for mass spectrometric analysis, 60 μg total protein were subjected to electrophoresis as described previously and then stained with silver nitrate by incubation with 0·2 g/l $Na_2S_2O_3$ for 1 min followed by 1 g/l $AgNO_3$ for 20 min on ice, and washed with 20 g/l Na_2CO_3 containing 0·1% HCHO. A 24 cm Immobiline DryStrip (pI, 3–11) was also used for preparation. It was rehydrated with 200 μg secreted protein and isoelectrofocused (25 kVh), then placed on 12·5% SDS-PAGE gel and overlaid with hot agarose solution. The electrophoresis was performed at a constant current of 400 mA. The gel was stained with silver nitrate as described earlier. Three sets of secretion samples from different animals were applied to 2D-electrophoresis and analyzed.

Western blotting

Total proteins, 0·3 μg of each preparation of prostate secretion, were applied to SDS-PAGE (5–20% gel). Proteins were then transferred to a piece of Hybond-P polyvinylidene difluoride (PVDF) membrane (Amersham). The membrane was incubated with a monoclonal antibody to GAPDH (Ambion) at 1 μg/ml followed by a peroxidase-conjugated antibody to mouse IgG (MBL Co., Nagoya, Japan) at a dilution of 1:1000. Protein bands were detected using the ECL system (Amersham).

Mass spectrometry (MS)

The protein spots were excised from the polyacrylamide gel and silver nitrate was removed with 15 mM $K_3[Fe(CN)_6]$ and 50 mM $Na_2S_2O_3$. The gel pieces were incubated in distilled water for 1 h, incubated with CH_3CN for 10 min, and dried in a centrifuge-vacuum concentration system. Each gel piece was incubated with a 20 μl aliquot of 10 μg/ml trypsin solution (sequence grade, Sigma) for 30 min on ice. Excess trypsin solution was removed, and the gel piece was incubated overnight at 35 °C. To extract the digested peptides, 10 μl of 70% CH_3CN containing 0·1% trifluoroacetic acid were added to each gel piece. An aliquot of 0·5 μl of the extract solution was spotted onto a target plate for an UltraFlex mass spectrometer (Bruker Daltonics, Bremen, Germany) along with 0·5 μl of 10 mg/ml α-cyano-4-hydroxycinnamic acid (MS grade, Nacalai tesque Co., Kyoto, Japan). MS was performed using an accelerating voltage of 20 kV, with data acquisition between 1000 and 4000 Da. Some of the fragment peaks were further analyzed by MS/MS. The MS and MS/MS data were evaluated with Biotools software (Bruker Daltonics) in combination with a peptide mass fingerprinting analysis system, MASCOT version 2·1 (Matrix Science, London, UK). The peptide mass fingerprinting was performed based on mass spectroscopy protein sequence database (MSDB; Imperial College London, UK) and the nr database at the National Centre for Biotechnology Information (NCBInr; Bethesda, MD, USA) with terminal modifications of peptides set as fixed carbamidomethyl and flexible oxidation ends. The peptide mass tolerance was set to 0·3%.

Quantification of mRNAs by real-time RT-PCR

Total RNA was prepared from each lobe of the prostate with an RNA Isolation kit (Promega), and 2 μg total RNA were reverse transcribed as described previously (Fujimoto *et al.* 2004). An ABI Prism 7700 (Perkin–Elmer Life Sciences, Boston, MA, USA) was employed for quantitative measurement of cDNA using a QuantiTect Sybr Green PCR kit (Qiagen). Specific primer sets with a T_m of about 59 °C were designed for each mRNA (Table 1). Prior to quantitative analysis, PCR products were prepared separately and purified by gel electrophoresis. The DNA sequences were confirmed with a capillary DNA sequencer, ABI 310 (Perkin–Elmer Life Sciences). Extracted fragments were used as standards for quantification. The PCR conditions were 15 min of initial activation followed by 45 cycles of 20 s at 94 °C, 30 s at 58 °C, and 40 s at 72 °C. All mRNA contents were normalized with reference to β-actin mRNA.

Serum testosterone levels

Serum testosterone levels were measured with an ELISA kit, purchased from Neogen Corp. (Lexington, KY, USA).

Statistical analysis

Statistical comparisons were made using Student's *t*-test.

Results

1D-PAGE analysis

The secretory proteins from the VP, DLP, AP, and SV were treated with a de-glycosidation enzyme, PNGase F, and analyzed with SDS-PAGE (Fig. 2). In the VP, a broad band at 20–25 kDa was evidently the major band, and a 10 kDa band

Table 1 Quantitative PCR primers for mouse genes

	GenBank accession #	5′-Primer (5′→3′)	3′-Primer (5′→3′)
Genes			
91 kDa protein	AK035662	GGACCTTCCACAAGCGAACAT	GCACTCCTCCAGGTGTTCCTC
AGR2	M_011783	TTCATCACTTGGACGAATGCC	ACGTACTGGCCATCAGGAGAA
Calr	NM_007591	ACCGTGAAGCATGAGCAGAAT	TGTTGATCAGCACATTCTTGCC
EAPA2	AY528666	CCAGACAGGCAGAATTGGGTT	CTCCTCGGAATCTATATTGGCG
GRP78	NM_022310	TCTTGCCATTCAAGGTGGTTG	TTCTTTCCCAAATACGCCTCAG
IgBPLP	XM_620455	CTGTGAGTTGCCCGAGCCT	CACAATGGAGAACGCCTCCT
PDI	MUSPDIA	CGCAACAACTTTGAGGGTGA	TTGGGCAGGAACAGCAGAAT
PLCα	M73329	ATTGCACTGCCAACACAAACA	AACTGAAGCTGGTCCTGCTTG
Prdx6	BC013489	AGGACGCTAACAACATGCCTG	GTGCCTGTCAGCTGGAGAGAG
Probasin	AF005204	ACACTGCATGTGCTAGGCGT	TCCCACACAAAATGTGACGG
PSP94	U89840	CCAACGCTACTAGGCCTTTGA	GCCCACACGAAGCACATTTAC
SBP	NM_011321	TGGAACCCGGTCAGATAACTTT	TCGACCCCTTCTAACACCAAA
SPI-KT3	BC086887	AGAGGCTAGTTGCCATGATGC	GGACAGGCTCTATGCGTTTCC
SVS2	NM_009300	CAGAGCAGCTCCTCAGAGGG	TCTGGGTCATGTCACCACCA
ZnG	AF281658	CCCACAGGACATAGACCCCTT	CTCATGTCAGGCAGAGAGGGTA
β-Actin	X03765	CTGTCCCTGTATGCCTCTGGTC	TGAGGTAGTCCGTCAGGTCCC

seemed to be secondary. PNGase F treatment shifted the major band to a sharper 19 kDa band, while other bands were unaffected. The main band in the DLP appeared to be a broad band at 80–100 kDa, together with bands at 17 and 13 kDa. PNGase F digested the major band into two sharper bands of approximately 80 and 90 kDa, which showed lower staining intensities. The mobility of other bands was not changed much by PNGase F treatment, although some smear-like

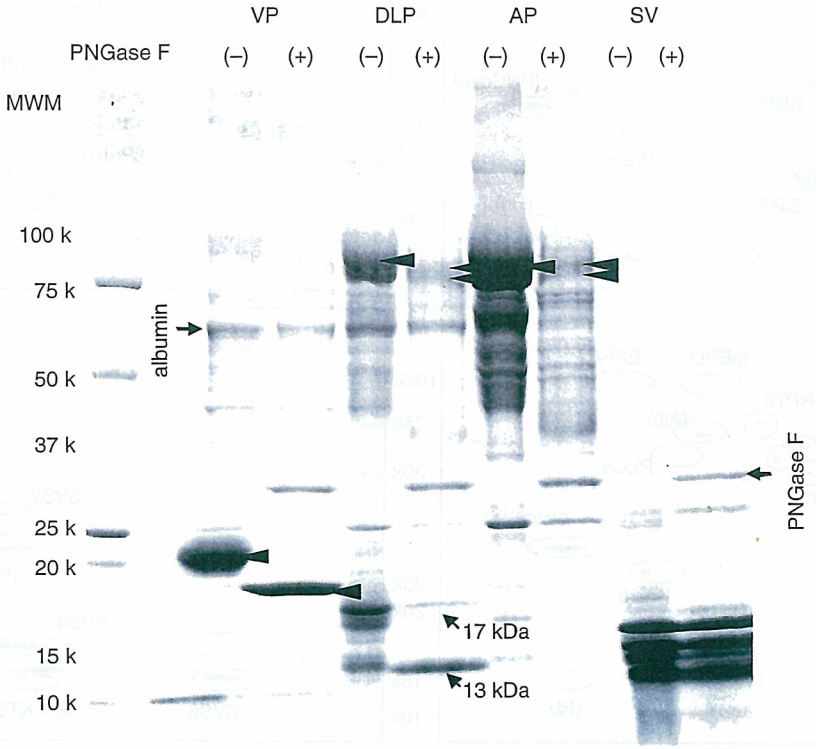

Figure 2 1D-SDS-PAGE analysis of mouse prostate secretory proteins. Secretion was prepared from the VP, DLP, and AP, as well as the SV. Each sample was incubated with (+) or without (−) PNGase F and applied to a 5–20% gradient SDS-PAGE gel. The gel was stained with Coomassie Brilliant Blue. Arrows indicate major shifted bands by PNGase.

staining disappeared. When the AP was compared with the DLP, the patterns of bands larger than 25 kDa were similar, as was the effect of PNGase digestion. However, several DLP-specific bands were present in the molecular weight range below 25 kDa. A band of albumin, 68 kDa, representing contamination from serum, was present in the preparations of prostatic secretion, especially in the VP and DLP. The pattern of SV protein bands was completely different from those of prostatic proteins. The major SV bands were observed between 10 and 16 kDa.

2D-PAGE and identified proteins

Secretory proteins from all the lobes were treated with PNGase F and subjected to 2D-PAGE analysis. Owing to the limitation in the pore size of the immobilized pH gradient gel for isoelectric focusing, proteins with a molecular mass of over 100 kDa could not be analyzed in the 2D-PAGE. Gels were stained and the major spots were picked up for MS analysis (Fig. 3). The analysis of three sets of prostate secretions from independent control mice provided identical patterns. The spots were successfully identified and the results were summarized in Table 2. SBP and SPI-KT3 were major proteins in the VP. In addition, a 91 kDa protein, predicted from urinary bladder cDNA data (AK035662) was identified in the VP, along with glucose-regulated protein 78 (GRP78 or heat-shock 70 kDa protein 5) and peroxiredoxin 6 (Prdx6). Two higher molecular weight proteins in the DLP and AP were identified as experimental autoimmune prostatitis antigen 2 (EAPA2) and a predicted protein similar to immunoglobulin-binding protein (immunoglobulin binding protein-like protein; IgBPLP). Zn-α2-glycoprotein (ZnG), a mammalian homologue of *Xenopus* anterior gradient 2 (AGR2), as well as PSP94 and probasin, were detected in the DLP secretion. Phospholipase Cα (PLCα), calreticulin (Calr), and protein disulfide isomerase were also identified in both DLP and AP secretions. SVS2, 4, 5, and 6 were identified in the SV fluid.

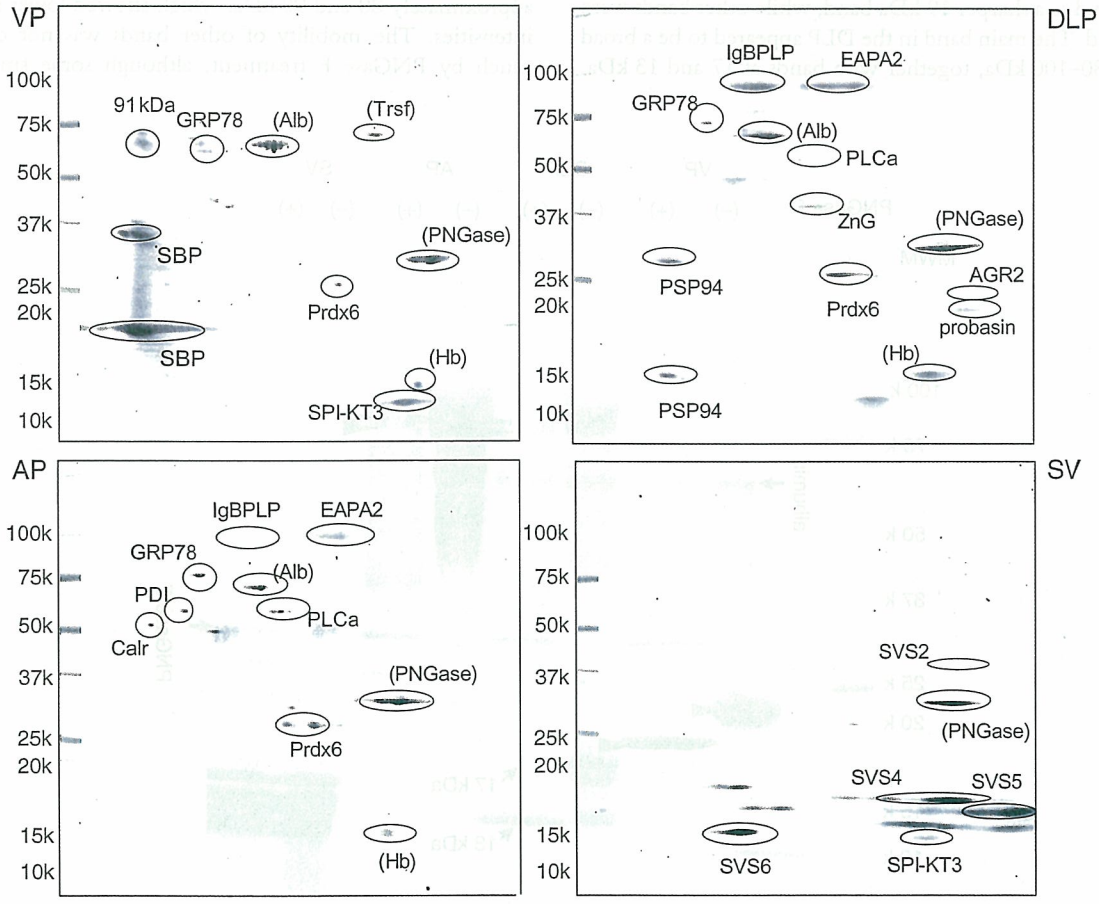

Figure 3 2D-PAGE analysis of mouse prostate secretory proteins. Each sample from the VP, DLP, AP, and SV was treated with PNGase F and applied to an immobilized pH gradient gel, followed by a second SDS-PAGE. Gels were stained with Sypro Ruby. The identified spots are indicated in the figure. Serum albumin (Alb), transferrin (Trsf), and hemoglobin (Hb) were considered to be due to serum contamination.

Table 2 Identified mouse prostatic secretory proteins

Abbreviation	Protein name	Accession #	Observed MW/pI	Theoretial MW/pI	*P*	Sequence coverage (%)
SBP	Spermine-binding protein	NP_035451	18,35/4·5	22/4·6	0·999	46
91 kDa	Protein predicted from cDNA AK035662	Q8BZE1	80/4·5	93/4·8	0·973	13
GRP78	Glucose-regulated protein 78 kDa	A37048	70/5·0	72/5·0	1·000	39
Prdx6	Peroxiredoxin 6	O08709	25/6·0, 6·5	25/5·6	1·000	57
SPI-KT3	Serine protease inhibitor, KT3	NP_033284	10/7·5	9/8·0	1·000	40
PSP94	Prostatic-secretory protein 94	NP_065622	13,28/5·0	13/5·5	1·000	76
IgBPLP	IgG-binding protein-like protein	XP_620455	100/ 5·5	210/5·5	1·000	28
EAPA2	Experimental autoimmune prostatitis antigen 2	NP_98193	100/6·5	103/6·2	1·000	42
PLCα	Phospholipase Cα	AAA39944	55/6·0	57/6·0	1·000	29
ZnG	Zinc-α2-glycoprotein	Q64726	35/6·0	34/5·8	0·992	28
AGR2	Homolog of *Xenopus* anterior gradient 2	BAB25181	20/9·5	20/9·5	1·000	56
Probasin	Probasin	AAC01954	22/9·5	21/10·1	1·000	56
Calr	Calreticulin	NP_031617	50/4·5	48/4·2	1·000	35
PDI	Protein disulfide isomerase	AAA39906	60/5·0	57/4·6	0·972	35

Lobe-specific mRNA expression of identified secreted proteins

Expression of identified proteins in the prostate was further confirmed by examining the mRNA levels; the results are summarized in Table 3. Lobe-specific expression of secreted proteins was evident. Both SBP and SPI-KT3 mRNAs were extremely abundant in the VP but virtually undetectable in the other lobes. The mRNA expression of the 91 kDa protein was also VP-specific. Abundant expression of IgGBPLP and EAPA2 mRNA was detected in the DLP and AP. Probasin expression was specific to the DLP/AP, while PSP94 mRNA was specific to the VP/DLP. The level of ZnG mRNA was highest in the DLP. The other protein mRNAs were expressed uniformly among the prostatic lobes.

Androgen dependency in mRNA expression of identified secreted proteins

Transcriptional regulation of identified proteins by androgen was examined by comparing mRNA levels among castrated, castrated plus testosterone-treated, and intact animals (Table 4). Serum

Table 3 mRNA levels of identified proteins in each prostatic lobe in 11-week-old mice

	SBP	SPIKT3	91 kDa	PSP94	ZnG	GRP78	AGR2
VP	511±58·9	184±36·0	3·6±0·8	2·6±0·6	0·9±0·1	1·7±0·5	0·14±0·03
DLP	0	0	0	5·8±1·5	12·3±1·1	6·1±1·7	0·38±0·04
AP	0	0	0	0	1·4±0·3	2·7±0·2	0·54±0·04
	PLCa	**Calr**	**PDI**	**Prdx6**	**Probasin**	**EAPA2**	**IgBPLP**
VP	0·17±0·021	0·7±0·1	15·0±2·1	2·5±0·3	0·06±0·02	0	0·0±0·0
DLP	0·36±0·085	1·2±0·3	8·3±2·1	21·7±2·6	2·15±0·23	18·9±1·5	67·9±10·3
AP	0·60±0·088	1·1±0·3	4·0±0·8	29·0±5·6	0·78±0·05	5·5±0·8	53·0±0·3

Means±S.E.M. (n=5). Values are mRNA levels divided by β-actin mRNA levels (mol/mol β-actin). 11-week-old male C57BL mice were killed and total RNA was isolated from each prostate lobe. mRNA levels were measured by real-time RT-PCR.

Table 4 Androgen regulation of mRNA levels of identified proteins

	SBP	SPIKT3	91 kDa	PSP94	ZnG	GRP78	AGR2
VP							
Cast	8·2±0·91[a]	0·24±0·08	0·09±0·02	0·011±0·004	0·38±0·032	0·57±0·36	0·03±0·004
Cast+T	48±7·9 (5·9)[b]	9·3±3·2 (39)	0·8±0·23 (8·4)	0·4±0·008 (38)	0·56±0·10 (1·5)	1·02±0·14 (1·8)	0·14±0·03 (4·9)
Intact	511±58·9 (62)	184±36 (769)	3·6±0·79 (40)	2·6±0·55 (236)	0·92±0·09 (2·4)	1·7±0·47 (3·0)	0·12±0·02 (4·3)
DLP							
Cast	–	–	–	0·002±0·001	0·64±0·11	0·55±0·11	0·01±0·001
Cast+T	–	–	–	0·08±0·046 (38)	2·0±0·48 (3·1)	3·4±0·73 (1·8)	0·06±0·02 (6·9)
Intact	–	–	–	5·8±1·48 (2633)	12·3±1·1 (19)	6·1±1·7 (11)	0·38±0·04 (45)
AP							
Cast	–	–	–	–	0·06±0·01	0·33±0·59	0·01±0·002
Cast+T	–	–	–	–	0·21±0·05 (3·6)	1·33±0·19 (4·1)	0·08±0·013 (9·5)
Intact	–	–	–	–	1·4±0·3 (24)	2·7±0·22 (8·3)	0·54±0·04 (64)

	PLCa	Calr	PDI	Prdx6	Probasin	EAPA2	IgBPLP
VP							
Cast	0·14±0·081	0·2±0·03	5·6±1·2	3·7±0·73	–	–	–
Cast+T	0·23±0·03 (1·6)	0·7+0·1 (3·3)	11·7±2·1 (2·1)	3·8±1·41 (1·0)	–	–	–
Intact	0·17±0·021 (1·2)	0·7+0·09 (3·5)	15·0±2·1 (2·7)	2·5±0·3 (0·7)	–	–	–
DLP							
Cast	0·09±0·014	0·2±0·05	1·7±0·32	1·5±0·41	0·02±0·003	0·19±0·072	1·2±0·29
Cast+T	0·15±0·02 (1·7)	0·3+0·07 (1·5)	4·5±1·0 (2·7)	2·1±0·22 (1·4)	0·05±0·002 (2·3)	2·4±0·55 (13)	1·6±0·6 (1·4)
Intact	0·36±0·085 (4·0)	1·2+0·3 (6·4)	8·3±2·1 (5·0)	21·7±2·6 (14)	2·2±0·23 (124)	18·9±1·5 (102)	67·9±10·3 (58)
AP							
Cast	0·20±0·03	0·4±0·06	1·4±0·3	1·2±0·15	0·02±0·004	0·17±0·52	0·25±0·18
Cast+T	0·34±0·085 (1·7)	0·7±0·05 (1·8)	2·8±0·5 (2·0)	4·7±0·93 (4·0)	0·04±0·008 (2·6)	4·8±0·9 (29)	1·1±0·8 (4·4)
Intact	0·60±0·088 (3·0)	1·1±0·3 (2·8)	4·0±0·8 (2·8)	29·0±5·6 (25)	0·78±0·051 (49)	5·5±0·8 (33)	53·0±0·31 (215)

[a]Mean±S.E.M. (n=5). Values are mRNA levels divided by β-actin mRNA levels (mol/mol β-actin).
[b]Values in parenthesis are fold change in mRNA over the castrated.10-week-old male C57BL mice were castrated and maintained for a week (cast). They were killed 24 h after testosterone administration at 5 mg/kg bw, ip (Cast+T). Total RNA was isolated from each prostate lobe and amounts of mRNA were measured by real-time RT-PCR.

testosterone levels were 0, 5·2±0·15, and 1·5±0·15 ng/ml in castrated, castrated plus testosterone injected, and intact groups respectively. Serum testosterone levels reached 38 ng/ml, 1 h after a testosterone injection. The mRNA levels of identified secreted proteins decreased 1 week after castration, although the extent of the decrease differed among protein species. For instance, SPI-KT3 mRNA in the VP was greatly decreased in castrated animals to only 1/769 of the intact control level, while castration reduced SBP expression to 1/62 of the control. The extent of change in mRNA expression also varied between lobes. GRP78 mRNA in the DLP, for instance, was decreased to 1/11 of the control by castration but only to about 1/3 of the control in the VP. The mRNA levels were normalized by β-actin levels, which were not affected by castration and testosterone treatment. The β-actin levels in the VP were 3·5±0·36, 3·8±0·30, and 3·5±0·34 fg/ng total RNA in the castrated, the castrated plus testosterone and intact groups respectively. The values were 4·8±0·74, 5·3±0·99, and 4·3±0·40 for the DLP, and 3·9±0·24, 4·2±0·60, and 4·7±0·26 for the AP.

Ontogeny in mRNA expression of identified secreted proteins

The expression of identified secreted protein mRNAs was examined in each lobe of the prostate at ages 1, 2, 4, 6, and 11 weeks (Table 5). Low levels of mRNA expression were noted at 1 week. Significant increases of SBP and EAPA2 mRNAs began at 2 weeks and continued thereafter. Increases in other secretory protein mRNAs, including 91 kDa protein, PSP94 and IgGBPLP mRNAs, were apparent at 4 weeks.

Discussion

In the present study, the major secretory proteins of the mouse VP, DLP, and AP were identified by mass spectrometric analysis after 2D-gel electrophoresis (Table 6). IgBPLP and EAPA2 were major proteins in the DLP/AP. A 91 kDa protein predicted from a mouse urinary bladder cDNA (AK035662), Prdx6 and PLCα were also found in the prostatic secretion for the first time, in addition to previously reported prostatic proteins, including SBP (Mills *et al.* 1987*b*), SPI-KT3 (Mills *et al.* 1987*a*), PSP94 (Xuan *et al.* 1999), and probasin (Johnson *et al.* 2000). The mRNAs for these proteins were expressed in a lobe-specific manner and were regulated by androgen. Our study has delineated the main mouse prostatic secretion pattern for the first time. The data will be useful for studying androgen-dependent gene regulation in the prostate, and may also provide markers for studying functional differentiation of prostate tissue.

Production and secretion of prostatic proteins are the main physiological functions of the prostate gland. Prostatic secretory proteins have been studied in rats as well as in humans, especially from the viewpoint of androgen-dependent regulation of expression and to identify possible markers of prostate cancer. The major human prostatic-secreted proteins are PSA (prostate-specific antigen), PSP94, and prostatic acid phosphatase (Lee *et al.* 1986). In rat, the composition of prostatic proteins is different; only PSP94 is common with the human case, and the production of each protein varies among lobes. In the VP, prostatic-binding protein or prostatein is the major secreted protein, while cystatin-related protein and kallikreins are also produced abundantly (Heyns 1990). The LP and DP secrete probasin,

Table 5 Ontogeny of mRNA levels of identified proteins in the prostate

	SBP	91 K	PSP94	EAPA2	IgBPLP
VP					
1W	0·1±0·04	0·1±0·02	0·1±0·05	–	–
2W	17·9±3·8*	0·1±0·01	0·2±0·08	–	–
4W	78·5±15·3*	0·8±0·07†	2·6±0·23†	–	–
6W	503·0±106*	3·6±0·23†	16·0±3·9†	–	–
11W	474·9±77·3*	4·4±0·50†	4·2±0·6†	–	–
DLP					
1W	–	–	0·0±0·03	0·18±0·06	0·05±0·02
2W	–	–	0·0±0·01	0·42±0·06*	0·09±0·02
4W	–	–	1·1±0·32*	0·88±0·27	0·68±0·21
6W	–	–	12·7±1·5†	3·95±0·79*	7·43±1·5*
11W	–	–	4·0±0·2†	15·3±2·36†	102±22·0†
AP					
1W	–	–	–	0·18±0·04	0·04±0·01
2W	–	–	–	0·74±0·02*	0·1±0·02
4W	–	–	–	1·10±0·4	1·9±0·26†
6W	–	–	–	3·55±0·53†	30·1±3·6†
11W	–	–	–	5·50±0·80†	53·2±8·1†

Means±S.E.M. (n=4). Values are mRNA levels divided by β-actin mRNA levels (mol/mol β-actin) 1, 2, 4, 6 and 11-week-old (W) male C57BL mice were killed. Total RNA was isolated from each prostate lobe and amounts of mRNA were measured by real-time RT-PCR. *P<0·05 and †P<0·01 vs. 1W.

Table 6 Summary: identified mouse prostatic secretory proteins

	Lobe specificity	mRNA decrease by castration	Description
Abbreviation			
SBP	VP	++	Known prostatic protein (Mills *et al.* 1987*b*)
SPI-KT3	VP, (SV)	+++	Known prostatic protein (Mills *et al.* 1987*a*)
91 kDa	VP	++	Scavenger receptor cys-rich (SRCR) domains
PSP94	VP, DLP	+++	Known prostatic protein (Xuan *et al.* 1999)
ZnG	DLP > VP, AP	+	Ribonuclease activity?
GRP78	VP, DLP, AP	+	Heat-shock protein 70 family
AGR2	VP, DLP, AP	+	Human homolog expressed in prostatic cancer cell lines
PLCa	VP, DLP, AP	+	Enzyme involved in phosphatidylinositol metabolism
Calr	VP, DLP, AP	+	Calcium-binding protein
PDI	VP, DLP, AP	+	Enzyme involved in protein folding
Prdx6	DLP, AP > VP	++	Antioxidant protein
Probasin	DLP, AP	+++	Known prostatic protein (Johnson *et al.* 2002)
EAPA2	DLP, AP	+++	No homology with any known protein
IgBPLP	DLP, AP	+++	IgG binding? Willebrand factor D domains, trypsin inhibitor like

PSP94, and SVS2 (Imasato *et al.* 2001). A kinesin heavy chain-like protein and an IgG-binding protein were recently reported in the secretion of the AP (Esposito *et al.* 2001, Wilhelm *et al.* 2002).

In spite of the morphological similarity of the prostate in mouse and rat, previous studies have suggested a substantial difference in prostatic secretion between the two species (Donjacour *et al.* 1990). Since mouse prostatic proteins are known to be highly glycosylated, we first examined the effects of glycosidase digestion on prostatic proteins. Endo H glycosidase, which cleaves mainly within the chitobiose core of high mannose, did not change the SDS-PAGE pattern (data not shown). On the other hand, PNGase F, which removes all types of N-linked glycosylation, changed the pattern. A broad band of SBP in the VP was converted to a sharp band with smaller molecular weight, and smear-like bands between 40 and 100 kDa in the DLP/AP were also converted to sharper bands, indicating that proteins were de-glycosylated by the enzyme. In spite of highly glycosylated characteristics of mouse prostate proteins, the biological role of glycosylation is not yet understood.

In the mouse prostate, only VP-secreted proteins have been investigated, and two major proteins, SBP and SPI-KT3, were identified (Mills *et al.* 1987*a*,*b*). The present study confirmed the secretion of these two proteins and also revealed the presence of other proteins, including 91 kDa protein, Prdx6 and GRP78. The 91 kDa protein is expected to consist of 841 aa with two predicted extracellular (CUB) domains and three scavenger receptor cystine-rich (SRCR) domains, and is expressed preferentially in the VP. The size of the protein, however, seems to be less than 91 kDa in the gel. Since the sequence coverage of peptide mass fingerprinting is only 13%, the actual reading frame may be shorter than the predicted one. Prdx6 is another new component of the prostatic secretion found in the present study. Since it is an antioxidant enzyme that reduces peroxide and alkyl hydroperoxide to water and alcohol respectively (Wang *et al.* 2003), it may provide seminal plasma antioxidant capability. GRP78 belongs to the heat-shock protein 70 family, which had been considered as intercellular proteins. However, a recent proteomic analysis of human prostasomes revealed the presence of heat shock proteins in prostatic secretion (Utleg *et al.* 2003). In addition, heat-shock protein 70 has been reported to be secreted from a variety of prostatic cell lines, and to show growth-inhibitory activity (Jones *et al.* 2004, Wang *et al.* 2004). Secreted mouse GRP78 may have a similar activity.

Although mouse DLP proteins had not been biochemically identified, Cunha's group has recognized 110 and 55 kDa bands in SDS-PAGE as major DLP/AP proteins (Donjacour *et al.* 1990). They reported that DLP/AP proteins are highly glycosylated, which was confirmed by the present study. The predicted IgGBPLP sequence derived from the cDNA sequence (XM_620455), however, is calculated to contain 1866 aa with a molecular mass of 201 kDa. Because peptide sequencing by the peptide-mass fingerprinting method covered the whole predicted sequence (27% coverage), the 100 kDa spot probably contains a mixture of cleaved fragments derived from the 201 kDa protein, although this remains to be confirmed. Recently, an IgG-binding protein of 115 kDa was reported to be secreted also from the rat AP, suggesting that a rat homolog exists (Wilhelm *et al.* 2002). The predicted cDNA sequence corresponding to this rat protein (XM_620455), which became available more recently, encodes 206 kDa protein (1914 aa) instead of 115 kDa. There is 84% similarity between the mouse and the rat sequences. Secretion of EAPA2, which is one of the antigens found in experimental autoimmune prostatitis, is also a noteworthy finding in the present study. This protein of 914 aa contains no known domain structure and has no homology with any known functional protein. Secretion of both PSP94 and probasin was detected in the DLP, as expected, since both proteins are well characterized in rats and have been reported in mice (Xuan

et al. 1999, Johnson *et al.* 2000). The other identified DLP proteins include GRP78, Prdx6, ZnG, AGR2, Calr, and protein disulfide isomerase (PDI). Prostatic secretion of ZnG has been reported in humans, and ZnG is widely distributed in body fluids and in various epithelia (Lei *et al.* 1998, Hale *et al.* 2001). AGR2 is a mammalian homolog of *Xenopus* AGR2, which was recently reported to be secreted from human prostate under androgen regulation (Zhang *et al.* 2005). It is overexpressed in prostate cancer and the expression level is correlated with pathological grade. Calr is a highly conserved calcium-binding protein involved in a wide variety of cellular processes (Krause & Michalak 1997). Interestingly, the Calr gene was identified as an androgen-inducible gene in the rat VP (Zhu *et al.* 1998). PDI is involved in the maintenance of folding of synthesized proteins. Specific expression of PDI in the prostate was recently reported in humans (Lexander *et al.* 2005). Since both Calr and PDI are considered to be localized in the lumen of endoplasmic reticulum, they may represent contaminants introduced during preparation of the secretion sample. Secretion from the AP is similar to that from the DLP, i.e. the major secretory proteins are IgGBPLP and EAPA2, but little ZnG and no PSP94 are found in the secretion. The results of mass spectrometric identification of SV proteins were generally in agreement with previous reports, i.e. SVS2, 4, 5, and 6, as well as SPI-KT3 (Lai *et al.* 1991, Lundwall *et al.* 1997). Except SPI-KT3, SV proteins are specifically expressed in the SV and not in the prostate gland, which differs from the rat case, where SVS2, for instance, is highly expressed in DLP/AP.

Quantitative determination of mRNA expression revealed a clear transcriptional differentiation of secreted proteins among the lobes. The levels of secretory protein mRNAs were very high, ranging from 1 to 500 times that of the housekeeping gene β-actin, used as an internal control in the present study. The mRNA levels overall correlated with the intensity of protein staining in the gel, although spots of protein with larger molecular weight, such as EAPA2 and IgBPLP show lesser intensity in the 2D-gel, since the 1D-gel used in the present study is only able to hold proteins with molecular weights less than 80–100 kDa. Since all the identified secreted proteins decreased significantly a week after castration of the animal, these protein transcripts are androgen-dependent directly or indirectly through involution of the gland. In rats, various studies have shown a faster response of the VP to androgen action, as compared with other lobes. For instance, castration decreased probasin mRNA expression to 1% of the control level after a week, while the decrease in the DLP was only 50% (Imasato *et al.* 2001). In the mouse, however, large decreases in mRNAs were evident in all the lobes. We examined the effect of a single injection of testosterone on the mRNAs in castrated animals to confirm the androgen dependency of transcription. The serum testosterone level well exceeded the control level within 1 h and was still high 24 h after an injection. Although most mRNA levels increased significantly after an injection, which clearly demonstrates their androgen inducibility, most of them were not restored to the intact control level. It may suggest that the full activity of androgen-dependent genes in the prostate is involved in both short- and long-term transcriptional regulation mechanisms by androgen.

Although rodent prostate models have been used for investigating the mechanism of prostate carcinogenesis, anatomical differences between rodent and human prostate have led to concerns about the validity of rodents as suitable models for human prostate cancer. Besides, mice are resistant to induction of prostate tumors by chemical carcinogens. However, a number of transgenic or knockout mouse lines have become available in which prostate carcinomas preferentially occur. For instance, the TRAMP transgenic line expresses the SV40 antigen under the control of the rat probasin promoter. The TRAMP mice develop high-grade prostatic intraepithelial neoplasia and prostate cancer within 12 weeks of birth, and ultimately develop metastases to the regional lymph nodes and lung by 30 weeks. In addition, androgen depletion by castration results in decreased tumor incidence. Their futures are similar to the human case, although metastasis to bone, a characteristic feature of human prostate cancer, is rare. The expression pattern of secretion proteins may be related to development of prostate carcinogenesis. Since the present study has revealed mouse prostate secretion, these can now be examined in relation to the development of prostate carcinogenesis as well as androgen-dependent differentiation of the gland. The ontogeny of mRNA expression of secreted proteins indicated that significant expression started 2 weeks after birth, which is consistent with the fact that branching morphogenesis of the mouse prostate is completed in the first 15 days of birth.

The present study has provided an understanding of the major secretory function of the mouse prostate, and identified common aspects of secretory functionality between mouse and human, e.g. for heat-shock proteins, ZnG and peroxiredoxin. The identified secretory proteins should be available as models of androgen-dependent gene regulation and are candidates as markers for prostatic differentiation. Like human PSA or PSP94, some of the identified proteins may be useful as pathological markers associated with prostate disorders; this would facilitate prostate research in mouse models.

Acknowledgements

We thank Ms R Tai for her expert technical assistance and Dr S Izumi for his expert suggestions for mass spectrometry. This work was supported in part by a Grant-in-Aid (H16-Seikatsu) from the Ministry of Health, Labor and Welfare, Japan and a Grant-in-Aid (#17510046) from the Ministry of Education, Culture, Sports, Science and Technology, Japan. The authors declare that there is no conflict of interest that would prejudice the impartiality of this scientific work.

References

Abate-Shen C & Shen MM 2002 Mouse models of prostate carcinogenesis. *Trends in Genetics* **18** S1–S5.

Cunha GR, Donjacour AA, Cooke PS, Mee S, Bigsby RM, Higgins SJ & Sugimura Y 1987 The endocrinology and developmental biology of the prostate. *Endocrine Reviews* **8** 338–362.

Donjacour AA, Rosales A, Higgins SJ & Cunha GR 1990 Characterization of antibodies to androgen-dependent secretory proteins of the mouse dorsolateral prostate. *Endocrinology* **126** 1343–1354.

Esposito C, Mariniello L, Cozzolino A, Amoresano A, Orru S & Porta R 2001 Rat coagulating gland secretion contains a kinesin heavy chain-like protein acting as a type IV transglutaminase substrate. *Biochemistry* **40** 4966–4971.

Fujimoto N, Igarashi K, Kanno J, Honda H & Inoue T 2004 Identification of estrogen-responsive genes in the GH3 cell line by cDNA microarray analysis. *Journal of Steroid Biochemistry and Molecular Biology* **91** 121–129.

Greenberg NM, DeMayo F, Finegold MJ, Medina D, Tilley WD, Aspinall JO, Cunha GR, Donjacour AA, Matusik RJ & Rosen JM 1995 Prostate cancer in a transgenic mouse. *PNAS* **92** 3439–3443.

Hale LP, Price DT, Sanchez LM, Demark-Wahnefried W & Madden JF 2001 Zinc alpha-2-glycoprotein is expressed by malignant prostatic epithelium and may serve as a potential serum marker for prostate cancer. *Clinical Cancer Research* **7** 846–853.

Heyns W 1990 Androgen-regulated proteins in the rat ventral prostate. *Andrologia* **22** (Suppl 1) 67–73.

Imasato Y, Onita T, Moussa M, Sakai H, Chan FL, Koropatnick J, Chin JL & Xuan JW 2001 Rodent PSP94 gene expression is more specific to the dorsolateral prostate and less sensitive to androgen ablation than probasin. *Endocrinology* **142** 2138–2146.

Johnson MA, Hernandez I, Wei Y & Greenberg N 2000 Isolation and characterization of mouse probasin: an androgen-regulated protein specifically expressed in the differentiated prostate. *Prostate* **43** 255–262.

Jones EL, Zhao MJ, Stevenson MA & Calderwood SK 2004 The 70 kilodalton heat shock protein is an inhibitor of apoptosis in prostate cancer. *International Journal of Hyperthermia* **20** 835–849.

Klein RD 2005 The use of genetically engineered mouse models of prostate cancer for nutrition and cancer chemoprevention research. *Mutation Research* **576** 111–119.

Krause KH & Michalak M 1997 Calreticulin. *Cell* **88** 439–443.

Lai ML, Chen SW & Chen YH 1991 Purification and characterization of a trypsin inhibitor from mouse seminal vesicle secretion. *Archives of Biochemistry and Biophysics* **290** 265–271.

Lee C, Tsai Y, Sensibar J, Oliver L & Grayhack JT 1986 Two-dimensional characterization of prostatic acid phosphatase, prostatic specific antigen and prostate binding protein in expressed prostatic fluid. *Prostate* **9** 135–146.

Lei G, Arany I, Tyring SK, Brysk H & Brysk MM 1998 Zinc-alpha 2-glycoprotein has ribonuclease activity. *Archives of Biochemistry and Biophysics* **355** 160–164.

Lexander H, Franzen B, Hirschberg D, Becker S, Hellstrom M, Bergman T, Jornvall H, Auer G & Egevad L 2005 Differential protein expression in anatomical zones of the prostate. *Proteomics* **5** 2570–2576.

Lundwall A, Peter A, Lovgren J, Lilja H & Malm J 1997 Chemical characterization of the predominant proteins secreted by mouse seminal vesicles. *European Journal of Biochemistry* **249** 39–44.

Maddison LA, Sutherland BW, Barrios RJ & Greenberg NM 2004 Conditional deletion of Rb causes early stage prostate cancer. *Cancer Research* **64** 6018–6025.

McPherson SJ, Wang H, Jones ME, Pedersen J, Iismaa TP, Wreford N, Simpson ER & Risbridger GP 2001 Elevated androgens and prolactin in aromatase-deficient mice cause enlargement, but not malignancy, of the prostate gland. *Endocrinology* **142** 2458–2467.

Mills JS, Needham M & Parker MG 1987*a* A secretory protease inhibitor requires androgens for its expression in male sex accessory tissues but is expressed constitutively in pancreas. *EMBO Journal* **6** 3711–3717.

Mills JS, Needham M & Parker MG 1987*b* Androgen regulated expression of a spermine binding protein gene in mouse ventral prostate. *Nucleic Acids Research* **15** 7709–7724.

Omoto Y, Imamov O, Warner M & Gustafsson JA 2005 Estrogen receptor alpha and imprinting of the neonatal mouse ventral prostate by estrogen. *PNAS* **102** 1484–1489.

Robertson FG, Harris J, Naylor MJ, Oakes SR, Kindblom J, Dillner K, Wennbo H, Tornell J, Kelly PA, Green J *et al.* 2003 Prostate development and carcinogenesis in prolactin receptor knockout mice. *Endocrinology* **144** 3196–3205.

Shirai T, Takahashi S, Cui L, Futakuchi M, Kato K, Tamano S & Imaida K 2000 Experimental prostate carcinogenesis – rodent models. *Mutation Research* **462** 219–226.

Utleg AG, Yi EC, Xie T, Shannon P, White JT, Goodlett DR, Hood L & Lin B 2003 Proteomic analysis of human prostasomes. *Prostate* **56** 150–161.

Wang X, Phelan SA, Forsman-Semb K, Taylor EF, Petros C, Brown A, Lerner CP & Paigen B 2003 Mice with targeted mutation of peroxiredoxin 6 develop normally but are susceptible to oxidative stress. *Journal of Biological Chemistry* **278** 25179–25190.

Wang MH, Grossmann ME & Young CY 2004 Forced expression of heat-shock protein 70 increases the secretion of Hsp70 and provides protection against tumour growth. *British Journal of Cancer* **90** 926–931.

Weihua Z, Makela S, Andersson LC, Salmi S, Saji S, Webster JI, Jensen EV, Nilsson S, Warner M & Gustafsson JA 2001 A role for estrogen receptor beta in the regulation of growth of the ventral prostate. *PNAS* **98** 6330–6335.

Wennbo H, Kindblom J, Isaksson OG & Tornell J 1997 Transgenic mice overexpressing the prolactin gene develop dramatic enlargement of the prostate gland. *Endocrinology* **138** 4410–4415.

Wilhelm B, Keppler C, Henkeler A, Schilli-Westermann M, Linder D, Aumuller G & Seitz J 2002 Identification and characterization of an IgG binding protein in the secretion of the rat coagulating gland. *Biological Chemistry* **383** 1959–1965.

Xuan JW, Kwong J, Chan FL, Ricci M, Imasato Y, Sakai H, Fong GH, Panchal C & Chin JL 1999 cDNA, genomic cloning, and gene expression analysis of mouse PSP94 (prostate secretory protein of 94 amino acids). *DNA and Cell Biology* **18** 11–26.

Zhang JS, Gong A, Cheville JC, Smith DI & Young CY 2005 AGR2, an androgen-inducible secretory protein overexpressed in prostate cancer. *Genes, Chromosomes and Cancer* **43** 249–259.

Zhu N, Pewitt EB, Cai X, Cohn EB, Lang S, Chen R & Wang Z 1998 Calreticulin: an intracellular Ca^{++}-binding protein abundantly expressed and regulated by androgen in prostatic epithelial cells. *Endocrinology* **139** 4337–4344.

Received 4 January 2006
Received in final form 24 April 2006
Accepted 26 May 2006
Made available online as an Accepted Preprint
13 June 2006

A POSSIBLE MECHANISM FOR THE DECREASE IN SERUM THYROXINE LEVEL BY POLYCHLORINATED BIPHENYLS IN WISTAR AND GUNN RATS

Yoshihisa Kato [1], Shin-ichi Ikushiro [2], Rie Takiguchi [1], Sekihiro Tamaki [1], Koichi Haraguchi [3], Toshiyuki Sakaki [2], Shizuo Yamada [1], Jun Kanno [4] and Masakuni Degawa [1]

[1] *School of Pharmaceutical Sciences, University of Shizuoka, 52-1, Yada, Suruga-ku, Shizuoka 422-8526, Japan*
[2] *Biotechnology Research Center, Faculty of Engineering, Toyama Prefectural University, 5180 Kurokawa, Imizu, Toyama, 939-0398, Japan*
[3] *Daiichi College of Pharmaceutical Sciences, 22-1, Tamagawa-cho, Minami-ku, Fukuoka 815-8511, Japan*
[4] *Division of Cellular & Molecular Toxicology, National Institute of Health Sciences, 1-18-1, Kamiyoga, Setagaya-ku, Tokyo 158-8501, Japan*

Introduction

Most polychlorinated biphenyl (PCB) congeners are known to decrease the levels of serum thyroid hormone and to increase the activities of hepatic drug-metabolizing enzymes in rats [1,2]. As possible mechanisms for the PCB-mediated decrease in level of serum thyroid hormone, enhancement of thyroid hormone metabolism by PCBs and displacement of the hormone from serum transport proteins (transthyretin (TTR)) are considered [3-5]. Especially, the decrease in the level of serum thyroxine (T_4) by 3,3',4,4',5-pentachlorobiphenyl, Aroclor 1254, and 2,3,7,8-tetrachlorodibenzo-*p*-dioxin in rats is thought to occur mainly through the induction of the UDP-glucuronosyltransferase (T_4-UDP-GT) responsible for glucuronidation of T_4 [2,4]. However, the magnitude of decrease in level of serum total T_4 is not necessarily correlated with that of increase in T_4-UDP-GT activity [1,6]. Recently, we suggested that the decrease in serum total T_4 level by a single administration of either Kanechlor-500 (KC500) or 2,2',4,5,5'-pentachlorobiphenyl in UGT1A-deficient Wistar rats (Gunn rats) was not dependent on the increase in hepatic T_4-UDP-GT activity, and further suggested that even in Wistar rats, the PCB-mediated decrease in serum T_4 level might occur not only through the increase in hepatic T_4-UDP-GT [7]. In the environment, humans and animals are exposed to PCB of very low level extent over a long period of time.

In the present study, therefore, to clarify possible mechanisms for the PCB-mediated decrease in level of serum thyroid hormone, we examined a relationship between the decrease in serum total T_4 level and the increase in the hepatic T_4-UDP-GT (UGT1A1 and UGT1A6) by the consecutive treatment of Wistar and Gunn rats with PCB and demonstrated that the PCB-mediated decrease in serum total T_4 level in rats was not necessarily dependent on the increase in hepatic T_4-glucuronidation, but the decrease occurs through the increased transport of T_4 to the liver.

Materials and Methods

Animal treatments. Male Wistar rats (160-200 g) and Gunn rats, (180-210 g) were obtained from Japan SLC., Inc. (Shizuoka, Japan). Male Wistar and Gunn rats were housed in three or four per cage with free access to commercial chow and tap water, and were maintained on a 12-h dark/light cycle (8:00 a.m.-8:00 p.m. light) in an air-controlled room (temperature: 24.5 ± 1℃, humidity: 55 ± 5%), and were handled with humane care under the guidelines of the University of Shizuoka (Shizuoka, Japan). The rats were treated with ip injection of KC500 (10 mg/kg) dissolved in Panacete 810 (5 ml/kg) at 24 h-intervals for 10 days. Control animals were treated with vehicle alone (5 ml/kg).

A) *In vivo* study. Rats were killed by decapitation on day 4 after the final dosing, and the liver was removed, and hepatic microsomes were prepared according to the method of Kato *et al.*[8] and stored at –85℃ until used. Blood was collected from each animal between 10:30 and 11:30 a.m. After clotting at room

temperature, serum was separated by centrifugation and stored at –50℃ until used.

Analysis of serum hormones. The levels of total T_4, free T_4, and thyroid-stimulating hormone (TSH) were measured by radioimmunoassay using the T4-RIABEAD (DAINABOT Co., Ltd, Tokyo, Japan), free T_4 (Diagnostic Products Corporation; Los Angels, CA), and Biotrak rTSH [^{125}I] assay systems (Amersham Life Science Ltd.; Little Chalfont, UK), respectivery.

Hepatic microsomal UDP-GT assay. The amount of protein was determined by the method of Lowry *et al.*[9] with bovine serum albumin as a standard. The activity of microsomal UDP-GT toward T_4 was determined by the method of Barter and Klaassen [3]. The UDP-GT activity was measured after activation of the UDP-GTs by 0.05% Brij 58.

Western blot analysis. Polyclonal anti-peptide antibodies against the common region of UGT1A isoforms and specific antibodies against UGT1A1, UGT1A6, and UGT2B1 were used [10]. Western analyses for microsomal UGT isoforms were performed by the method of Luquita *et al.*[11]

B) *Ex vivo* study. At 4 day after last treatment with KC500, animals were anesthetized with 50 mg/ml sodium pentobarbital combined 1:1 with 1 mg/ml potassium iodide at 2 mg/ml. The femoral artery was cannulated and primed with heparinized saline. Fifteen minutes later, animals were given [^{125}I]T_4 i.v. at 15 μCi/ml in 10 mM NaOH saline including 1 % normal each animal serum.

Clearance of [^{125}I]T_4 from serum. Five minutes following i.v. administration of [^{125}I]T_4 and five more times at the indicated time, a portion of blood was sampled from the artery, and serum was collected and stored at -50℃ for assay. Two aliquots were taken from serum samples for γ-counting.

Analysis of [^{125}I]T_4 binding to serum proteins. The levels of serum [^{125}I]T_4-albumin, [^{125}I]T_4-thyroxine binding protein, and [^{125}I]T_4-TTR complexes were determined by the method of Kato *et al.*[12]

Tissue distribution of [^{125}I]T_4. At 60 min after the administration of [^{125}I]T_4, blood was sampled from abdominal aorta, and tissues were removed and weighted. Radioactivities in serum and tissues were determined by γ-counting, and concentration ratios of the tissue to serum were determined.

Results and Discussion

The serum total T_4 and free T_4 levels were markedly decreased not only in the Wistar rats but also in the Gunn rats 4 days after final treatment with KC500 (10 mg/kg, i.p., once daily for 10 days), and there was no significant difference in magnitude of the decrease between Wistar and Gunn rats (Fig. 1). At the same time, the level and activity of T_4-UDP-GT (UGT1A1 and UGT1A6) were significantly increased by treatment with KC500 in Wistar rats but not in Gunn rats (Fig. 2). In contrast, the level of UGT2B1 was increased by KC500 in both Wistar and Gunn rats. Hepatic microsomal enzyme activities (benzyloxyresorufin *O*-dealkylase activity, 48- and 35-fold; pentoxyresorufin *O*-dealkylase activity (CYP2B1/2), 17- and 10-fold; ethoxyresorufin *O*-dealkylase activity (CYP1A1/2), 64- and 10-fold in Wistar and Gunn rats, respectively) were significantly increased by KC500 treatment. In addition, no significant change in the level of serum TSH by the KC500 treatment was observed in either Wistar or Gunn rats.

Furthermore, significant increases in the disappearance of [^{125}I]T_4 from the serum and in the distribution volume of [^{125}I]T_4 by KC500 treatment were observed in both Wistar and Gunn rats. A concentration ratio of the liver to serum was approximately one in either Wistar or Gunn rats, and KC500-treatment increased the ratio by 4 times. The concentration of [^{125}I]T_4 appeared to be the highest in the liver in both Wistar and Gunn rats. The hepatic levels of [^{125}I]T_4 in both rats were further increased by KC500 treatment. More than 40% of [^{125}I]T_4 dosed was transported to the liver of both rats (Fig. 3). In contrast, a significant increase in liver weight was observed in KC500-treated Wistar rats but not in the Gunn rats. In addition, significant decrease in the binding of [^{125}I]T_4 to serum TTR and significant increase in the binding to serum albumin by KC500 treatment were observed in either Wistar or Gunn rats.

In conclusion, the present findings demonstrate that the PCB-mediated decrease in serum total T_4 level in Gunn rats occurs without an increase in hepatic T_4-UDP-GT activity; they further suggest that in both strain rats, the PCB-mediated decrease occurs through the increased transportation of T_4 to the liver. Furthermore, the decrease in the binding of T_4 to serum TTR and hepatic hyperplasia might be attributed to the increase in the level of T_4 in the liver. In Wistar rats, however, the PCB-mediated induction of T_4-UDP-GT might, at least in part, contribute to the decrease. Further studies are necessary for understanding the susceptibility toward a PCB-mediated decrease in serum T_4 level in animals including humans.

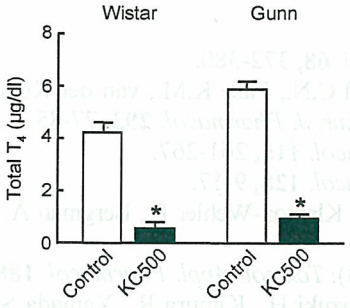

Fig. 1. Effect of KC500 on the level of serum total thyroxine in Wistar and Gunn rats

Animals were killed 4 days after the final administration of KC500 (10 mg/kg, i.p., once daily for 10 days). Each column represents the mean ± S.E. (vertical bars) for five to six animals. *P<0.01, significantly different from each control.

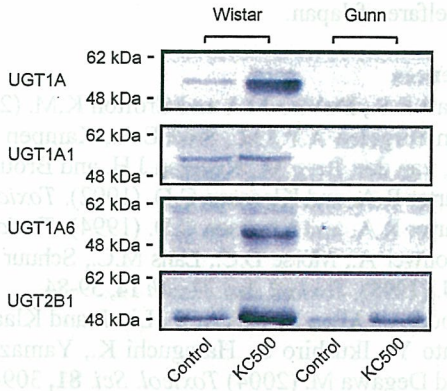

Fig. 2. Representive Western blot patterns for hepatic microsomal UGT isoforms in KC500-treated Wistar and Gunn rats

Animals were killed 4 days after the final administration of KC500 (10 mg/kg, i.p., once daily for 10 days).

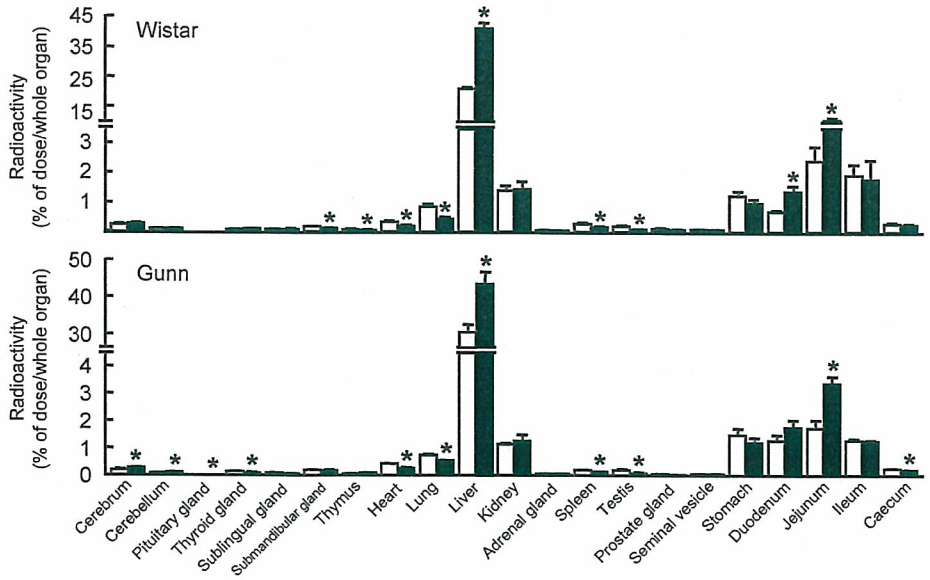

Fig. 3. Tissue distribution of total radioactivity after the administration of [^{125}I]T_4 to the KC500-treated Wistar and Gunn rats

KC500 (10 mg/kg) was given i.p. to animals at 24 hr-intervals for 10 days. The radioactivity of each tissue was measured at 60 min after the i.v. administration of [^{125}I]T_4. Each column represents the mean ± S.E. (vertical bars) for three to six animals. *P<0.05, significantly different from each control. ☐, control; ■, KC500.

Acknowledgements

This work was supported in part by the Grant-in-Aid for Scientific Research (C) (no. 18510061, Y.K.) from Japan Society for the Promotion of Science, and by a Health and Labour Sciences Research Grant for Research on Risk of Chemical Substances (H16-Kagaku-003, Y.K.) from the Ministry of Health, Labour and Welfare of Japan.

References

1. Craft E.S., DeVito M.J. and Crofton K.M. (2002). *Toxicol. Sci.* **68,** 372-380.
2. van Birgelen A.P.J.M., Smit E.A., Kampen I.M., Groeneveld C.N., Fase K.M., van der Kolk J., Poiger H., van den Berg M., Koeman J.H. and Brouwer, A. (1995). *Eur. J. Pharmacol.* **293,** 77-85.
3. Barter R.A. and Klaassen C.D. (1992). *Toxicol. Appl. Pharmacol.* **115,** 261-267.
4. Barter R.A. and Klaassen C.D. (1994). *Toxicol. Appl. Pharmacol.* **128,** 9-17.
5. Brouwer A., Morse D.C., Lans M.C., Schuur A.G., Murk A.J., Klasson-Wehler E., Bergman Å. and Visser T.J. (1998). *Toxicol. Ind. Health* **14,** 59-84.
6. Hood A., Allen M.L., Liu Y., Liu J. and Klaassen, C.D. (2003). *Toxicol. Appl. Pharmacol.* **188,** 6-13.
7. Kato Y., Ikushiro S., Haraguchi K., Yamazaki T., Ito Y., Suzuki H., Kimura R., Yamada S., Inoue T. and Degawa M. (2004) *Toxicol. Sci.* **81,** 309-315.
8. Kato Y., Haraguchi K., Kawashima M., Yamada S., Masuda Y. and Kimura R. (1995). *Chem.-Biol. Interact.* **95,** 257-268.
9. Lowry O.H., Rosebrough N.J., Farr A.L. and Randall R.J. (1951) *J. Biol. Chem.* **193,** 265-275.
10. Ikushiro S., Emi Y. and Iyanagi T. (1995). *Arch. Biochem. Biophys.* **324,** 267-272.
11. Luquita M.G., Catania V.A., Pozzi E.J.S., Veggi L.M., Hoffman T., Pellegrino J.M., Ikushiro S., Emi Y., Iyanagi T., Vore M. and Mottino A.D. (2001). *J. Pharmacol. Exp. Ther.* **298,** 49-56.
12. Kato Y., Suzuki H., Ikushiro S., Yamada S. and Degawa M. (2005). *Drug Metab. Dispos.* **33,** 1608-1612.

Drug Metab. Pharmacokinet. 21 (1): 70–74 (2006).

Regular Article

Monospecific Antipeptide Antibodies Against Human Hepatic UDP-Glucuronosyltransferase 1A Subfamily (UGT1A) Isoforms

Shin-ichi IKUSHIRO[1], Yoshikazu EMI[2], Yoshihisa KATO[3], Shizuo YAMADA[3] and Toshiyuki SAKAKI[1]

[1]*Biotechnology Research Center, Faculty of Engineering, Toyama Prefectural University, Toyama, Japan*
[2]*Graduate School of Life Science, University of Hyogo, Hyogo, Japan*
[3]*School of Pharmaceutical Sciences, University of Shizuoka, Shizuoka, Japan*

Full text of this paper is available at http://www.jstage.jst.go.jp/browse/dmpk

Summary: Expression of UDP-glucuronosyltransferases (UGT) in mammals is thought to be regulated in both a tissue- and developmental-specific manner. Furthermore, induction of genes encoding UGT occurs after exposure to xenobiotics including drugs, environmental pollutants and dietary compounds. In human, isoforms of UGT 1A subfamily catalyze the glucuronidation of a greater proportion of drugs, suggesting that the expression of UGT1A isoforms is responsible for the clearance of a diverse range of drugs. To analyze the expression of human UGT1A isoforms, we have developed polyclonal antibodies against specific peptide regions within the isoforms (UGT1A1, 1A3, 1A4, 1A6 and 1A9). The prepared antipeptide antibodies were found to be highly monospecific for each UGT1A isoform and no cross-reactivity with UGT2B isoforms was detected. Analysis of UGT1A protein levels in hepatic microsomes using these antibodies demonstrated interindividual differential expression of each isoform. These highly specific antipeptide antibodies provide an important tool to analyze tissue distribution and interindividual expression levels of human UGT1As.

Key words: antipeptide antibody; glucuronidation; humanUGT1A isoform; liver microsomes

Introduction

UDP-glucuronosyltransferases (UGTs, EC 2.4.1.17), which are located mainly in the endoplasmic reticulum, play a major role in the detoxification of drugs and other xenobiotics including environmental pollutants and dietary compounds in all vertebrates.[1)] UGTs catalyze the transfer of glucuronic acid to the hydroxyl, carboxyl, sulfhydryl or amine groups of structurally unrelated compounds, resulting in the formation of water-soluble glucuronides for excretion in the bile or urine. Mammalian *UGTs* can be classified, according to their substrate specificity, sequence similarity and gene structure, into three subfamilies: *UGT1*, *UGT2* and *UGT3*.[2)] Many of the UGT isoforms have been identified and characterized in terms of their substrate specificity after expression of the corresponding cDNA in heterologous cells.[3)]

In human liver, five UGT1A cDNAs have been identified and characterized: UGT1A1, 1A3, 1A4, 1A6 and 1A9.[4)] Although the expression of different UGT isoforms at the mRNA level in hepatic and extrahepatic tissues has been quantified, there is a paucity of protein data for each isoform due to the lack of specific antibodies. Without a detailed knowledge of the relevant protein levels it is difficult to accurately determine the contribution of specific UGT isoforms to the metabolism of the liver and other tissues. Therefore, the development of isoform-specific antibodies is needed to fully characterize the protein level of each UGT in major tissues and to define the substrate specificity for each UGT isoform. We have developed isoform-specific antipeptide antibodies to rat UGT isoforms and characterized inducer-dependent induction and tissue specific expression.[5–9)] In this report, we developed human UGT1A isoform-specific antipeptide antibodies to analyze the expression of the isoforms in hepatic microsomes. These highly specific antibodies provide an important tool to study tissue distribution and cellular expression levels of UGT isoforms.

Received; October 6, 2005, Accepted; November 24, 2005
To whom correspondence should be addressed: Shin-ichi IKUSHIRO, *Tel. +81-766-56-7500 (ext 566), Fax. +81-766-56-2498, E-mail: ikushiro@pu-toyama.ac.jp*

Table 1. Amino acid sequences of antigen peptides for human UGT1A isoforms

Isoforms	Positions	Sequences
UGT1A	520–533	KKGRVKKAHKSKTH
UGT1A1	108–121	RVIKTYKKIKKDSA
UGT1A3	82–100	ISWTQDEFDRHVLGHTQLY
UGT1A4	107–120	LKRYSRSMAIMNNV
UGT1A6	82–95	YDQEELKNRYQSFG
UGT1A9	102–115	VRSIYSLLMGSYND

Methods

Materials: Human hepatic microsomes from 5 individual livers (HH13, HH18, HK25, HG43 and HG89) were purchased from BD Biosiences (Woburn, MA). Informed consents for the preparation of the microsomes were obtained from all donors. Recombinant human UGT1A1, UGT1A3, UGT1A4, UGT1A6, UGT1A7, UGT1A8, UGT1A9, UGT1A10, UGT2B4, UGT2B7, UGT2B15 and UGT2B17 expressed in baculovirus-infected insect cells (Supersomes) were also purchased from BD Biosciences. All other chemicals were of the best commercially available grade.

Preparation of anti-peptide antibodies: The amino-terminal half of each human UGT1A, deduced from the corresponding cDNA sequence, was selected for the preparation of human UGT1A isoform-specific antipeptide antibodies (**Table 1**). The carboxyl-terminal region (14 aa) of UGT1A, which is common to all UGT1A isoforms, was selected for preparing anti-UGT1A antibodies. An additional cysteine residue was included at the amino-terminus of each peptide sequence to facilitate conjugation to a carrier protein, Keyhole limpet hemocyanin (KLH). The synthetic peptides (14–19 aa) were conjugated with KLH *via* the amino-terminal cysteine using maleimidobenzoyl-N-hydroxysuccinimide.[5] Rabbits were immunized with the KLH-peptide conjugates emulsified in Freund's complete adjuvant. Subcutaneous immunization (250 μg KLH-peptides per rabbit) was performed three times, at 2 week intervals, and the rabbits were bled two weeks after the third injection. The antisera titers were monitored by ELISA assay using synthetic peptides conjugated with bovine serum albumin as a standard. The antipeptide antibodies were purified from antisera by using the corresponding peptides coupled to a BrCN-activated Sepharose 4B column. Six monospecific antipeptide antibodies against human UGT1A isoforms were generated corresponding to the sequence of UGT1AC, UGT1A1, 1A3, 1A4, 1A6 and 1A9, which were designated h1AC, h1A1, h1A3, h1A4, h1A6 and h1A9, respectively.

Immunoblot analysis: SDS-polyacrylamide gel electrophoresis (PAGE) was performed using a 4% (w/v) stacking and a 10% (w/v) separating gel.[5] The proteins in the gel were blotted to nitrocellulose membranes using a semi-dry blotting method. The membranes were washed in distilled water and blocked at 25°C for 1 hour in blocking buffer (50 mM Tris-HCl pH 8.0, 150 mM NaCl, 1.5% (w/v) bovine serum albumin), followed by incubation with diluted antibodies (1:1000–1:6000 dilution) at 25°C for 15 hours. The membranes were washed in PBS containing 0.05% (v/v) Tween 20 and incubated with a 1:5000 dilution of alkaline phosphatase-conjugated goat anti-rabbit IgG (CTS. Inc., MA, USA) at 25°C for 2 hours. Immunodetection was developed by adding 1.7 mg/mL bromochloroindolyl phosphate and 0.7 mg/mL nitro blue tetrazolium. The band intensity of the blot sheet was quantitated using densitometric scanner with high resolution and NIH image software (Version 1.61). Endoglycosidase H (EndoH) treatment under denaturing conditions was performed as follows. A 20 μL aliquot of sample used for the SDS-PAGE analysis was directly subjected to EndoH treatment (200 units) for 60 min at 37°C. The reaction was terminated by heating at 98°C for 5 min.

Results and Discussion

The human *UGT1A* gene cluster spans more than 200 kb of chromosome 2 and is organized in a unique arrangement.[2] A series of divergent first exons are located consecutively over 150 kb, each encoding approximately 280 aa. The 3′ region of the locus comprises exons 2–5, which encode the conserved 245 aa carboxyl terminal region of UGT1A. The amino- and carboxyl-terminal halves of UGT are thought to be involved in the recognition/binding of substrate and UDP-glucuronic acid, respectively.[5] Because the UGT1A isoforms share a very high level of overall sequence identitiy (66–93%), it has proved difficult to prepare isoform-specific antibodies. Previously, we have successfully developed specific antipeptide antibodies against rat UGT1A isoforms and demonstrated that the isoforms are independently induced by various xenobiotics.[5–9] In this work, a peptide-specific antibody strategy was chosen to raise specific antibodies against human UGT isoforms.

A comparative analysis of the amino acid sequence of human UGT isoforms identified unique regions for designing peptides for isoform-specific antibody preparation (**Table 1**). UGT1A peptide is located at the carboxyl-terminal end of all UGT1A isoforms, but is distinct from the sequence found in UGT2B isoforms. The isoform-specific peptides were unique to each isoform and corresponded to the hypervariable region I (residues 60–150) of UGT1, which is thought to be involved in aglycon recognition.[10] Affinity-purified antibodies were tested for specificity by immunoblot

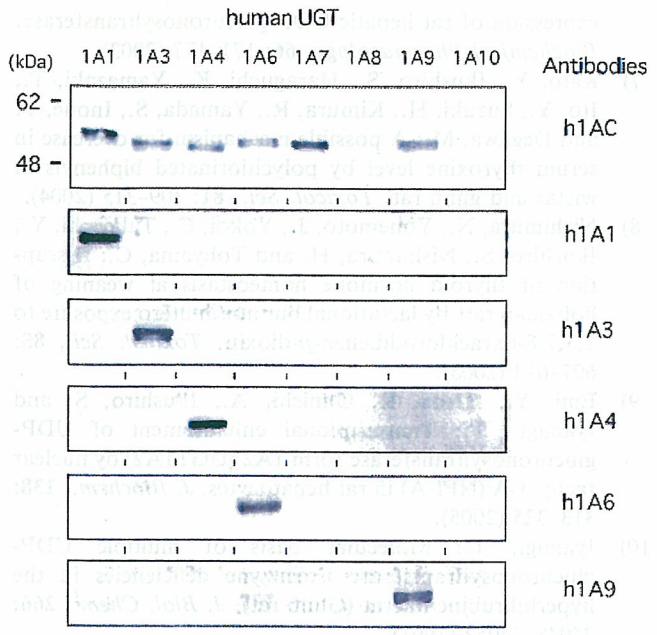

Fig. 1. Immunospecificity of anti-UGT1A isoform-specific peptide antibodies. Approximately 1 μg of microsomes containing recombinant human UGT1A isoforms was used for the analysis of h1AC and 5 μg for each UGT1A isoform-specific antibody preparation.

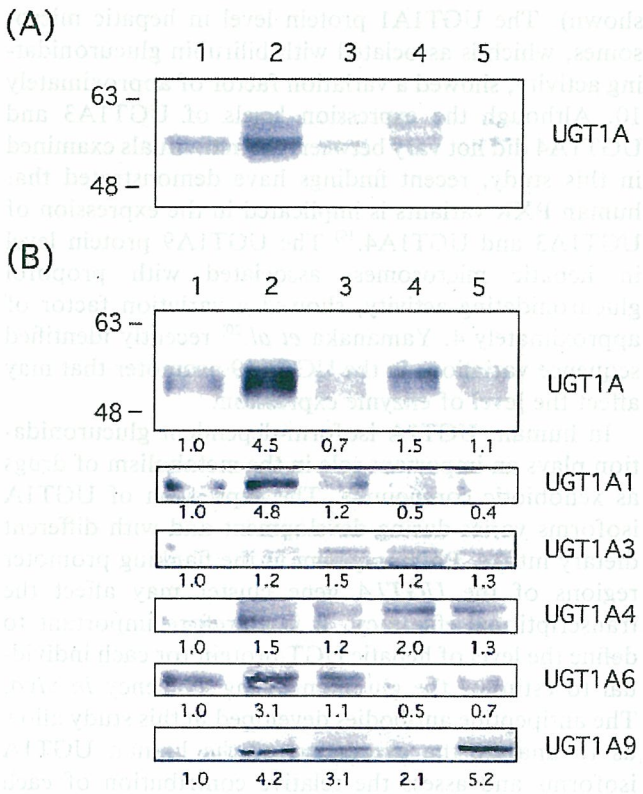

Fig. 2. Analysis of interindividual expression of human UGT1A isoforms in hepatic microsomes using specific antibodies. Commercially available human hepatic microsomes from 5 individuals were used: lane 1; HH13, lane 2; HH18, lane 3; HK25, lane 4; HG43, lane 5; HG89. Hepatic microsomes were untreated (A) or treated (B) with endoglycosidase H. Approximately 20 and 40 μg of microsomes was used for the analysis of h1AC and isoform-specific antibodies, respectively. Values of each panel represent the relative expression level of UGT isoforms in hepatic microsomes.

analysis of commercially available recombinant human UGTs. The antipeptide antibodies against each UGT1A isoform displayed highly specific immunoreactivity (**Fig. 1**). Furthermore, these antibodies did not recognize human UGT2B isoforms UGT2B4, 7, 15 and 17 (data not shown).

Despite the high level of sequence identity between UGT1A3 and 1A4 (93%), h1A3 and h1A4 only reacted with the corresponding isoform. Recently, Iwai *et al.*[11] used an antipeptide antibody preparation against UGT1A3 to detect the recombinant enzyme in an expression system, but did not verify the antibody specificity. Girard *et al.*[12] and Miles *et al.*[13] developed an antibody against the N-terminus of recombinant UGT1A9 protein to determine the protein content of UGT1A9 in human liver microsomes. However, the antibodies recognized closely related UGT1A isoforms, UGT1A7, 1A8 and 1A10, in addition to UGT1A9. Our antipeptide antibody, h1A9, did not recognize UGT1A7, 1A8 and 1A10, indicating that the expression level of hepatic UGT1A9 protein could be determined without cross-reactivity against related UGT1A isoforms.

Recently, several lines of evidence indicate significant interindividual variability in *UGT1A* expression and the associated glucuronidating activity. Genetic variations in the promoter region of each isoform affect the expression of the corresponding protein. Polymorphism of the UGT1A1 promoter region is known to be associated with disorders of bilirubin metabolism and an adverse effect to SN-38.[14] In addition to genetic variation, regulation of the UGT1 locus is under selective transcriptional control with a number of xenobiotic and steroid receptors.[15–18] Antipeptide antibodies were used to determine the UGT protein levels in a panel of human hepatic microsomes. A considerable degree of heterogeneity in UGT1A expression in individuals is evident from the cross-reactivity of h1AC with several bands (**Fig. 2, panel A**). Treatment of microsomes with endoglycosidase H resulted in a shift of these bands, indicating the modification of UGT1A isoforms with high mannose-type sugar chains (**Fig. 2, panel B**). Furthermore, different patterns of expression of UGT1A isoforms between individuals was detected using the isoform-specific antibodies. Because the levels of NADH-cytochrome b_5 reductase and NADPH-cytochrome P450 reductase do not vary between individuals, these microsomal proteins were used as a convenient control for our experiments (data not